

## **Effect of Noise Stress on Lung and Heart of the Adult Albino Rats and the Possible Protective Role of Sulpiride.**

**Tamer M. M. Abu-Amara<sup>1\*</sup>, Gamal S. Elgharabawi<sup>1</sup>, Moustafa E. E. Motawee<sup>1</sup>, Salah E. Mourad<sup>2</sup>, Neama M. Taha<sup>3</sup>.**

<sup>1</sup>Histology&Cytology Department, College of Medicine, Al-Azhar University, Egypt.

<sup>2</sup>Anatomy Department, College of Medicine, Al-Azhar University, Egypt.

<sup>3</sup>Physiology Department, College of Medicine, Umm Al-Qura University, KSA.

\*Corresponding author: Tamer M. M. Abu-Amara, Lecturer of Histology & Cytology Department, College of Medicine, Al-Azhar University, Egypt, E-mail: tamer4567@yahoo.com

### **Abstract**

Exposure to noise stress is associated with increased respiratory system morbidity; however the underlying mechanisms are unclear. Thus there is a need for more study about this harmful effect. Sulpiride had been shown to have a protective role against noise stress on other systems but this role did not studied well on respiratory system.

**Aim of the work:** To investigate using histological, histochemical and morphometric methods the possible harmful effects of noise on adult female albino rats' lung, heart and the possible protective role of combined sulpiride treatment.

**Material and Methods:** The present study was carried out on 24 adult female albino rats which were randomly divided into **Group 1(C, untreated negative control)**, **Group 2 (N, noise exposed or positive control)** where rats were exposed to noise ">90 decibel/3h/day" for 1 month, **Group 3(D, sulpiride treated)** where rats were exposed to sulpiride "0.028 mg/B.W./day" and **Group 4 (N+D, noise+ sulpiride exposed)**. Paraffin sections were prepared for histological, histochemical and morphometric study. Also statistical analysis was done.

**Results:** Rats exposed to noise only or sulpiride only showed highly significant damaging changes on lung such as thickening in the interalveolar septa and obliteration of the alveoli, inflammatory cells infiltration within the pulmonary interstitium, peribronchiolar infiltration and fibrosis, thickening of the pulmonary blood vessels walls, interstitial collagen fibres deposition and apoptotic cellular changes. On the level of heart, highly significant decrease in the diameters of the myocardial muscle fibres with focal areas of necrosis and apoptotic changes was detected. Also, increased collagen fibres deposition was marked in sulpiride group. When noise and sulpiride treatment was combined, the damaging effects were maximized on the lung and to a lesser extent on the heart.

**Conclusion:** These results provide evidence that noise stress cause obvious lung and heart tissue damages. No protective role for sulpiride was proofed. This is as using sulpiride alone or in combination with noise showed marked damaging effects on the lung and heart tissues.

**Keywords:** *Noise, Sulpiride, Albino rats, Lung, Heart, Stress, Histology and Histochemsitry.*

## Introduction

Stress is defined as the state in which the brain interprets the quantity of stimulation as excessive or its quality as threatening <sup>(1)</sup>. Exposure to hostile conditions (usually referred to as stressors) results in a series of important adaptive responses that enable an organism to cope with a changing environment <sup>(1)</sup>. Prolonged repeated stress can be extremely harmful <sup>(2, 3)</sup>. Stress stimulates several adaptive hormonal responses such as secretion of catecholamines from the adrenal medulla, corticosteroids from the adrenal cortex, and adrenocorticotropin from the anterior pituitary <sup>(4)</sup>. In fact, the sympato-adrenal and hypothalamic-pituitary-adrenocortical systems have complex interactions to maintain the internal environment during exposure of the organism to a wide variety of stressors <sup>(4, 5, 6)</sup>. Stress affects the psychological and physiological activities in human and can disrupt and threaten our internal homeostasis <sup>(7, 8)</sup>.

Noise is kind of stress which pervasive aspects resemble of many modern community and work environments. Acute noise exposure activate the autonomic and hormonal systems, leading to temporary changes such as increased blood pressure, increased heart rate and vasoconstriction after prolonged exposure, susceptible individuals in the general population may develop permanent effects, such as hypertension and ischemic heart disease that are associated with exposures to high sound pressure levels. Other drastic effects of noise include the impairments of rest, sleep and blood pressure <sup>(9)</sup>. The effects of noise on the immune system have also been reported <sup>(10)</sup>. Noise exposure over 90 decibel (dB) becomes a stressor and contributes to the genesis and manifestation of several multifactor diseases <sup>(11)</sup>.

Stress has been implicated as an environmental factor that may accelerate the process of biological aging and decline the functional integrity of system involved in the stress reaction <sup>(5)</sup>. Adaptation to stress can be the bases of some diseases. For instance, in humans and animals, several studies have shown that stress may induce type 1 & 2 diabetes mellitus <sup>(8, 12, 13, 14, 15)</sup>. Noise causes the release of stress hormones, which in turn affects the risk factor pattern for cardiovascular disease <sup>(16)</sup>.

Antidepressant drugs are the most successful in patients with clearly (vegetative) characteristics including psychomotor retardation, sleep disturbance, poor appetite and weight loss. However, a variety of chemical structures have been found to have antidepressant activity <sup>(17)</sup>. Sulpiride, a neuroleptic drug, from the group of benzamides, exerts antiautistic stimulating effects, has positive influence on productive symptoms of psychosis and shows antidepressant activity <sup>(18,19, 20, 21, 22)</sup>. Sulpiride is the most favorite drug which used to tolerate stress symptoms as it has relatively minor adverse effects <sup>(18)</sup>. Also, in comparison to many tricyclic antidepressant, sulpiride reaches its maximal blood concentration after 2-4 hours from oral administration <sup>(23, 24, 25)</sup>.

This work was done using histological, histochemical and morphometric methods to investigate two parameters. First parameter was to investigate the possible harmful effects of noise on the adult female albino rats' lung and heart. Second parameter was to investigate the possible protective role of combined sulpiride treatment.

## Material and Methods

**Animals:** 24 adult female albino rats weighing 150-200 gm were used in this study. They were kept under observation for one week before beginning of the experiment to acclimatize. During the 24 daily hours, animals were exposed to 14 hrs artificial light followed by 10 hrs complete darkness at normal atmospheric temperature. All animals were fed on standard diet contained protein, fibers, fats, carbohydrates, and supplied with vitamins and minerals mixture with continuous supply of water. Sulpiride drug was administered orally by gastric tube at a dose of 0.28mg/ 100gm body weight/day for one month. Sulpiride dose was calculated according to the Paget's formula on the basis of the human dose <sup>(26)</sup>. Noise was applied by exposure to 5 different sources of unharmonic and high intensity music.

**Study groups:** The animals were divided into 4 main groups. Each group contained 6 rats. Animals were categorized as the following:  
**Group 1 (C):** normal rats served as negative control (without any treatment for one month).

**Group 2 (N):** rats exposed to noise only for one month (>90 decibel, 3h/day). According to Brennan et al. <sup>(27)</sup> when noise exposure of any

kind exceeds 90 dB, noise becomes a stressor.

**Group 3 (D):** rats treated with the drug only for one month (0.028mg/g body weigh /day).

**Group 4 (N+D):** rats exposed to noise and treated with the drug for one month.

**Histological and histochemical study:** rats from the control and treated groups were sacrificed after month and small pieces of lung and heart were taken for the histological and histochemical studies. Specimens were prepared via fixation in 10% neutral buffered formol solution and Carnoy's fluid. Paraffin sections with 5µm thickness were prepared and stained with Harris haematoxylin and eosin <sup>(28)</sup>. Collagen fibers were stained by Mallory's trichome stain <sup>(29)</sup>. Polysaccharides were detected by PAS (Periodic acid-Schiff) method <sup>(29)</sup>. Total proteins were detected by mercuric bromophenol blue method <sup>(30)</sup>.

**Morphometric analysis:** The image analyzer (ImageJ 1.46r) was used to obtain the following morphometric data:

- The mean thickness of interalveolar septa using H&E stained sections at 400x magnification.
- The mean number of alveolar macrophages/ field using oil immersion lens in H&E stained sections at 1000x magnification.
- The percentage of collagen fibers in the lung alveoli using Mallory's trichrome stained sections at 400x magnification.
- The mean thickness of pulmonary vessels of lung interstitium using H&E stained sections at 400x magnification.
- The total protein in lung tissue using mercuric bromophenol blue sections at 400x magnification.
- The mean thickness of myocardial cells using H&E stained sections at 400x magnification.
- The percentage of collagen fibers in the myocardial muscle fibres using Mallory's trichrome stained sections at 400x magnification.

The previous measurements were estimated in five non-overlapping fields/section in five serial sections/rat from each animal in each group.

**Statistical analysis:** all statistical analysis was performed using the statistical software PAlentological Statistics Version 3.0 (PAST 3.0) <sup>(31)</sup>. The obtained data were expressed as mean±standard deviation (SD) and analyzed

using analysis of variance (ANOVA). Statistical significance level was defined as  $P < 0.05$ .

## Results

**The control group, Group 1 (C):** H&E stained sections of the lung tissue showed normal alveoli with thin interalveolar septa, clearly seen alveolar sacs, bronchiole with folded columnar epithelial cells and normal pulmonary vessels (Figs. 1A, 2A). The alveolar epithelium showed type I pneumocytes (extremely flattened with very thin cytoplasm and densely stained flattened nuclei) and type II pneumocytes (cuboidal cell with large dark stained rounded nuclei which are commonly located near the angles between neighbouring alveolar septa) (Fig. 3A).

Few number of macrophage cells was also detected in the lung interstitium (Fig. 3A). Mallory's trichome stained sections of lung tissue revealed normal distribution of thin collagen bundles in pulmonary interstitium around the alveolar sacs, in the interalveolar septa, around bronchioles and the pulmonary blood vessels (Fig. 4A).

PAS (Periodic acid-Schiff) stained sections of the lung tissue showed moderate PAS reaction (magenta red) in the basal lamina of alveolar epithelium, alveolar sacs and endothelium of pulmonary vessels as well as cytoplasm of epithelium lining bronchioles (Fig. 5A).

Mercuric bromophenol blue stained sections of the alveolar tissue showed normal distribution of total protein in the pulmonary interstitium, in the muscular layer of bronchioles and pulmonary blood vessels (Fig. 6A).

**Group 2 (N) and Group 3 (D):** H&E stained sections of the alveolar tissue showed obliteration of some alveoli with subsequent compensatory dilatation of others (Figs. 1B, 2B, 1C, 2C).

Highly increased thickness of the interalveolar septa ( $P < 0.001$ ) was detected (Figs. 1B, 2B, 1C, 2C, 12) (Tab.1). Cellular apoptotic changes such as pyknotic nuclei were detected in the lung interstitial cells (Figs. 3B, 3C).

Highly significant increase in both inflammatory cells infiltration within connective tissue surrounding lung bronchioles

( $P < 0.001$ ) and pulmonary blood vessels diameter ( $P < 0.001$ ) were also detected (**Figs. 1B, 2B, 1C, 2C, 14, 15**) (**Tab.1**).

Mallory's trichome stained sections of the lung tissue of group 2 showed highly significant deposition of collagen fibres ( $P < 0.001$ ) in bronchiole walls, peribronchiolar areas, interalveolar septa, and pulmonary blood vessels (**Figs. 4B,13**) (**Tab. 1**).

Group 3 showed similar results to group 2 with more collagen deposition around the blood vessels (**Figs. 4C,13**) (**Tab. 1**). PAS stained sections of the lung tissue of group 2 revealed strong PAS reaction in RBCs seen in the congested pulmonary vessels, endothelium of the pulmonary vessels and inflammatory cells infiltration (**Fig. 5B**).

Group 3 illustrated similar findings to noise exposed one. However, weak PAS reaction was observed in the perivascular areas and collapsed alveoli (**Fig. 5C**). Mercuric bromophenol blue stained sections of the lung tissue of both group 2 and 3 showed highly significant increase ( $P < 0.001$ ) in total protein content (deep stain in comparison to control) in the bronchiolar walls, peribronchiolar areas and the pulmonary blood vessels (**Figs. 6B, 6C, 16**) (**Tab. 1**).

**Group 4 (N+D):** H&E stained sections of the lung tissue showed marked obliteration of some alveoli with thickened interalveolar septa and subsequent compensatory dilatation of others (**Figs. 1D, 2D, 12**).

Marked thickening of the bronchiole walls, peribronchiolar infiltration with inflammatory cells and granulomatous formation were detected. Highly significant thickening of pulmonary blood vessels ( $P < 0.001$ ) was detected with marked perivascular infiltration and fibrosis (**Figs. 1D, 2D, 15**) (**Tab.1**).

More necrotic tissue and cellular pyknotic changes than group 2 and 3 had been shown (**Fig. 3D**).

High significant increase in both cellular infiltration within the connective tissue surrounding lung bronchioles and in the pulmonary blood vessels diameters ( $P < 0.001$  and  $< 0.001$  respectively) were also detected (**Figs. 1D, 2D, 14, 15**) (**Tab.1**). Mallory's trichome stained sections of the alveolar tissue

revealed marked highly significant increase in collagen fibers deposition ( $P < 0.001$ ) in bronchiole epithelial cells, submucosa, peribronchiolar area, in thick interalveolar septa and around the pulmonary blood vessels with marked thickening of their walls (**Figs. 4D,13**) (**Tab. 1**).

PAS stained sections of the alveolar tissue showed strong PAS reaction in endothelium of the pulmonary vessels, in perivascular areas, and in sites of interstitial cellular infiltration. Also, weak PAS reaction was observed in perivascular areas and collapsed alveoli (**Fig. 5D**).

Mercuric bromophenol blue stained sections of the alveolar tissue showed highly significant increase ( $P < 0.001$ ) in total protein content (deep stain in comparison to the control) in the bronchiolar walls, peribronchiolar areas and the pulmonary blood vessels (**Figs. 6D, 16**) (**Tab. 1**).

**The control group, Group 1 (C):** H&E stained sections of the cardiac muscle fibers illustrated branching and anastomosing cardiac muscle fibers with acidophilic sarcoplasm and central elongated vesicular nuclei of cardiomyocytes and the nuclei of fibroblasts in the interstitium (**Figs. 7A, 8A**).

Mallory's trichome stained sections of the cardiac muscle revealed few collagen fibers in-between the muscle fibers (**Fig. 9A**). PAS stained sections of the cardiac muscle revealed normal polysaccharides content (normal distribution of PAS+ve materials) in the cardiac tissue (**Fig. 10A**).

Mercuric bromophenol blue stained sections of the cardiac muscle revealed normal distribution of total protein in the cardiac tissue (**Fig. 11A**).

**Group 2 (N) and Group 3 (D):** H&E stained sections of the cardiac muscle fibers for group 2 illustrated some degenerative changes of the myocardial muscle fibers (**Fig. 7B**).

Group 3 showed myocardial cellular degenerative changes and inflammatory cells infiltration (**Fig. 7C**). Focal areas of necrotic muscle fibers with vacuolated cytoplasm, small deeply stained pyknotic nuclei and faintly stained karyolytic nuclei were detected in both group 2 and 3 (**Figs. 8B, 8C**).

Significant decrease in the diameter of myocardial muscle fibres in both group 2 and 3 ( $P < 0.05$ ,  $<0.05$  respectively) was detected (**Fig. 17**) (**Tab. 1**). Mallory's trichome stained sections of the cardiac muscle fibers of group 2 revealed few collagen fibers in between the muscle fibers with no significant difference in comparison to the control group (**Fig. 9B, 18**) (**Tab. 1**).

Group 3 showed high significant increase of collagen muscle fibers deposition ( $p < 0.01$ ) in comparison to the control group (**Fig. 9C, 18**). PAS stained cardiac muscle fibers of both group 2 and 3 revealed normal polysaccharides content (normal distribution of PAS+ve materials) in the cardiac muscle fibers (**Figs. 10B, 10C**). Mercuric bromophenol blue stained cardiac muscle fibers of both group 2 and 3 revealed reduced total protein (focal areas of faint stain affinity) in cardiac muscle fibers (**Fig. 11B, 11C**).

**Group 4 (N+D):** H&E stained sections of the cardiac muscle fibers showed marked myocardial cellular degenerative changes and inflammatory cells infiltration (**Fig. 7D**). More necrotic areas with vacuolated cytoplasm and small deeply stained pyknotic nuclei than group 2 & 3 were detected (**Fig. 8D**).

However, no significant change in myocardial cells has been proved in comparison to control group (**Tab. 1**). Mallory's trichome stained sections of the cardiac muscle fibers revealed marked highly significant deposition of collagen fibers ( $P < 0.001$ ) in bronchiolar epithelial cells, submucosa, peribronchiolar area and in thick interalveolar septa with cellular infiltration in interalveolar septa (**Figs. 9D, 18**) (**Tab. 1**).

Moderate amount of collagen fibers was detected around the blood vessels with marked thickening of the blood vessels (**Figs. 9D, 18**). PAS stained sections of the cardiac muscle fibers showed poorly stained (focal areas of decreased staining affinity of PAS stain) cardiac myocytes (**Fig. 10D**). Mercuric bromophenol blue stained sections of the cardiac muscle revealed marked reduction in total protein (faint stain affinity) content in the cardiac myocytes (**Fig. 11D**).

## Discussion

Noise stress had been shown to carry many negative drawbacks on various organs of our body. For instance, noise causes release of various stress hormones which in turn affects the risk factor pattern for cardiovascular and pulmonary diseases <sup>(16)</sup>. After prolonged exposure to noise, susceptible individuals may develop chronic diseases, such as hypertension and ischemic heart disease <sup>(9)</sup>. Long-term exposure to hypertension lead to congestive heart failure as it induces left ventricular remodelling and cardiac hypertrophy <sup>(32)</sup>.

Also, mechanical stress increase reactive oxygen species (ROS) production that leads to cardiomyocytes apoptosis and subsequent heart failure <sup>(11, 33)</sup>. Moreover, stress can cause hypertension and subsequent congestive heart failure via its damaging effects on kidney <sup>(32, 34)</sup>. Furthermore, effects of noise on the immune system have been reported and play a role in genesis and manifestation of several multifactor diseases <sup>(10)</sup>. Liver injury, inflammation and fibrosis after exposure to stress were reported <sup>(35)</sup>.

Our study showed that noise stress and sulpiride treatment caused remarkable histological and structural drawbacks on lung and heart tissues. Rats exposed to noise only or sulpiride only showed highly significant damaging changes on lung such as thickening in the interalveolar septa and obliteration of alveoli, inflammatory cells infiltration within pulmonary interstitium, peribronchiolar infiltration and fibrosis, thickening of the pulmonary blood vessels, interstitial collagen fibres deposition and apoptotic cellular changes.

On the level of heart, highly significant decrease in the diameter of myocardial fibers with focal areas of necrotic fibers and apoptotic changes were detected. Also, collagen fibres deposition was marked in sulpiride group. When noise and sulpiride treatment was combined, the damaging effects were maximized on the lung and to a lesser extent on the heart. **Eman et al.** <sup>(36)</sup> study showed similar effect for noise on kidney cortex, where highly thickened arterial walls and increased kupffer cells were detected. In our study, the Increased number of inflammatory cells may be due to and reflecting the active defense mechanism against the noise stress or the toxic effect of

sulpiride. **Zhang and Kaufman** <sup>(32)</sup> declared that the increase in Kupffer cells numbers reflect clearly the active defense mechanism against the toxic substances. Increased collagen fibers observed in our present study may lead to rapid healing as reported by **Zhang et al.** <sup>(37)</sup>. The increase in collagen fibers deposition under different stresses was observed by several authors <sup>(38, 39, 40, 41)</sup>. In this issue, **George et al.** <sup>(42)</sup> suggested that decreased synthesis of collagenolytic enzymes that might contribute to further accumulation of collagen. Thickened arterial walls observed in our study were also detected by other authors <sup>(34, 36, 43)</sup>.

Exposure to stress induces oxidative stress leading to increased free radical production which cause hypertrophy of both vascular smooth muscle cells and arterial walls hypertrophy <sup>(34, 43)</sup>. Our results showed increase total proteins content in lung in groups 2, 3 and 4, while cardiac muscle showed decrease in total proteins content in these groups. Altered collagen fibers, polysaccharides and total protein in the present study may be a result of elevated free radicals post-exposure to noise as reported in previous studies <sup>(11, 44)</sup>.

Also, decreased protein content after noise exposure was detected in brain in previous studies <sup>(11, 44)</sup>. In this issue, **Willis et al.** <sup>(45)</sup> demonstrated that stress inhibits protein synthesis by alteration in the balance between phosphorylation and dephosphorylation. When corticosteroids were administered acutely to normal fasting human, there is an increase of protein breakdown <sup>(46)</sup>. Decreased stain affinity of total protein observed in the present study can discuss the degeneration and fibrosis observed in heart tissue after noise exposure or sulpiride treatment. Thin degeneration was noticed in other studies due to injury of mitochondria, Golgi apparatus and DNA fragmentation <sup>(40, 47, 48)</sup>.

Different stressors can affect mitochondria leading to rupture of the outer mitochondrial membrane, release of the inner membrane components, apoptosis and finally induce cell death <sup>(49, 50)</sup>. Similar to the related previous studies, the histological changes of our study may result from an increase in the process of lipid peroxidation and decreased activity of antioxidant enzymes of the body with the consequent damage of cellular membranes <sup>(51, 52)</sup>.

The beneficial effects of sulpiride in treating some disorders were reported by several authors <sup>(53, 54, 55)</sup>. Also, previous studies such as **Eman et al.** <sup>(36)</sup> showed that sulpiride drug may play a protective role against noise stress negative drawbacks. However, our results showed that sulpiride has a harming effect on lung and heart tissues when it was used alone or in combination with noise.

In conclusion, our results provide evidence that noise stress cause obvious lung and heart damages. No protective role for sulpiride was proofed as using sulpiride showed marked damaging effects on the lung and heart.

## References

1. **Carrasco GA and Van de Kar LD (2003):** Neuroendocrine pharmacology of stress. **European Journal of Pharmacology**. 463: 235–272.
2. **Cyr NE (2009):** Identifying hormonal habitation in field studies of stress. **Gen .Comp. Endocrinol.** ,161: 295- 303.
3. **Liu J. Wisniewski M, Tian V, et al (2011):** Glycine betain improves oxidative stress tolerance and biocontrol efficacy of the antagonistic yeast *Cystofilobaidium*. **International Food Microbiology**. 121: 210-215.
4. **Sabban EL and Kvetnansky R (2010):** Stress-triggered activation of gene expression in catecholaminergic systems: dynamics of transcriptional events. **Trends in Neurosciences**. 24 (2): 91–98.
5. **Negrão AB, Deuster PA, Gold PW, Singh A, Chrousos GP, et al (2000):** Individual reactivity and physiology of the stress response. **Biomedical Pharmacotherapy**. 54 (3): 122–128.
6. **Tyler H, Shaw G, Matthews J, Warm S, Finomore, L.(2010):** Individual differences in vigilance: personality, ability and states of stress. **Journal of Research in Personality**. 44: 297-308.
7. **Swain MGI (2000):** Stress and hepatic inflammation. **Am. J. Physiol .Gastrointest Liver Physiol**. 279: 1135-1138.
8. **Maltos E, Tome S, Silva T, Maria D, et al (2011):** Effect of harvesting stress and storage

- conditions on protein degradation in fillets of formed gilthead sea bream: A differential scanning calorimetry study. **Food Chemistry**. 126:270-276.
9. **Tomoyuki H (2004):** Effect of noise on the health of children. **J. Nippon. Med. School**. 71:5-10.
  10. **Archana R, Namasivayam A (2000):** Effect of Ocimum sanctum on noise induced change in neutrophil function . **J. Ethnopharmacol**. 73: 81-85.
  11. **Samson T, Sheela D, Ravidran M, Senthilvelan A, et al (2005):** Effect of noise stress on free radical scavenging enzymes in brain. **Environmental toxicology and Pharmacology**. 20:142-148.
  12. **Stein SP, Charles E (2007):** Emotional factors in juvenile diabetes mellitus: a study in the early life experiences of adolescent diabetes. **The American Journal of Psychiatry**. 128 (6): 700–704.
  13. **Strommer L, Permert J, Arnelo U, Koehler C, Isaksson B, Larsson J, et al (2009):** Skeletal muscle insulin resistance after trauma: insulin signaling and glucose transport. **American Journal of Physiology** 275 (38): 351–358.
  14. **Frank T (2010):** Cultures as problem in linking material in equality to health: on residential crowding. **J. Pharmacology, Biochemistry and Behavior**. 16: 523- 530.
  15. **Soop M, Nygren J, Myrenfors P, Thorell A, Ljungqvist O, et al (2011):** Preoperative oral carbohydrate treatment attenuates immediate postoperative insulin resistance. **American Journal of Physiology, Endocrinology and Metabolism**. 280 (4): 576–583.
  16. **Colleen G, Le P, David F, Dolan D, Bennett Peter AB, et al (2009):** Nutrient plasma level achived during treatment that reduced noise induced hearing loss. **Translational Research**. 106:320-333.
  17. **Rosana C, Tania M, Elizabeth M, Yonamine MC, et al (2010):** Ethanol-induced sensitization dependspreferentially on D<sub>1</sub> rather than D<sub>2</sub> dopamine receptors. **Pharmacology, Biochemistry and Behavior**. 98: 173-180.
  18. **Jae-Jin K, Dae J, Tae-Gyun K, Jeong-Ho S, Ji-Won C, et al (2007):** Volumetric abnormalities in connectivity based subregions of the thalamus in patients with chronic schizophrenia. **Schizophrenia Research**. 97: 226-235.
  19. **Charles E (2011):** Psychopharmacology :house divided ,progress in neuro-psychopharmacology and biology. **Journal of Psychiatry**. 35:1-10.
  20. **Camarini R, Marcorkis T, Teodorv E, Maria H, et al (2011):** Ethanol-induced sensitization depends preferentially on D<sub>1</sub>rather thanD<sub>2</sub> dopamine receptors.J. **Biochemistry and Behavior**. 98: 173-180.
  21. **Mohammad N, Fatemeh M, Shahrbanoo O, Sima N, Mohammad R, et al (2011):** The effects of dopaminergic drugs in the dorsal hippocampus of mice in the nicotine-induced anxiogenic-like response. **Pharmacology, Biochemistry and Behavior**. 98: 468-473.
  22. **Mori K, Kim J, Sasaki K, et al (2011):** Electrophysiological effects of orexin–B and dopamine on rat nucleus accumbens shell neurons *in vitro*. **Peptides**. 32: 246-252.
  23. **Michal A, Ina W, (2008):** Fluctuation of latent inhibition along the estrous cycle in the rat: modeling the cyclicity of symptoms in schizophrenic women. **Journal of Psychoneuroendocrinology**. 33: 1401-1410.
  24. **Martin S, Cindy L, Stephan F, et al (2010):** Cholinergic contribution to the cognitive symptoms of schizophrenia and the viability of cholinergic treatment.J. **Neuropharmacology**. 34: 188-195.
  25. **Nikol F, Mira S, Christos R, et al (2005):** Canine versus in vitro data for predicting input profiles of 1- sulpiride after oral administration. **European Journal of Pharmaceutical Sciences**. 26: 324-333.
  26. **Paget GE, Barnes JM, (1964):** Evaluation of drug activityIn: Pharmaceutics Laurence and Bacharach, Vol.1 **Academic press. NewYork**.
  27. **Brennan FX, Job R, Watkins LR, Maier SF, et al (1992):** Total plasma cholesterol levels of rats are increased following only three sessions of tail shock. **Life Sci**. 50(13): 545-550.
  28. **Drury R, Wallington E (1980):** Carleton's Histological Technique. 4<sup>th</sup> Ed. **Oxford. Univ. Press, New York, Toronto**. Pp: 115-119.

29. **Pearse A (1977):** Histochemistry, Theoretical and Applied. 3<sup>rd</sup> Ed vol I. **Churchill Livingstone, London.** Pp: 112-115.
30. **Mazia D, Brewer P, Alfert M, et al (1953):** The cytochemical staining and measurement of protein with mercuric bromophenol blue. **Biol.Bull.** 104: 57-67.
31. **Hammer Ø, Harper DAT, Ryan PD, et al (2001).** PAST: Paleontological Statistics Software Package for Education and Data Analysis. **Palaeontologia Electronica.** 4(1): 9-15 Pp.
32. **Zhang K and Kaufman, RJ (2008):** From endoplasmic-reticulum stress to the inflammatory response. **Journal of Nature.** 454: 455-462.
33. **Katzung BG (2008):** Basic and Clinic Pharmacology, **Appleton and Lange, Lebanon,** Pp: 448–460.
34. **Agarwal MD (2005):** Hypertension in chronic kidney disease and dialysis : pathphysiology and management. **Cardiol. Clin.** 23: 237-248.
35. **Vere CC, Streba T, Ionescu G, et al (2009):** Psychosocial stress and liver disease status. **World Gastroenterology.** 28:2980-2986.
36. **Eman GH, Fatma E, Neama MT, et al (2011).** Protective effects of sulpiride treatment on kidney functions of female albino rats exposed to noise stress. **The Egyptian Journal of Hospital Medicine.** 44: 284 – 294.
37. **Zhang D, Xu Z, Chiang A, Lu D, Zeng Q, et al (2006):** Effect of GSM 1800 MHz radiofrequency EMF on DNA damage in Chinese hamster lung cells. **Zhonghuo Nei. Brain Research.** 916: 107–114.
38. **Shediwah F (2005):** Control of toxicity induced during chemotherapy and radiotherapy using natural plant substance. **Ph. D. Thesis, Zoology Department, Faculty of Science, Al- Azhar Univ. Cairo.**
39. **Al Gahtani S (2006):** Histological and histochemical studies on the effect of two different types of magnetic field on the liver and kidney of albino rats. **M.Sc. Zoology Department, Girls College of Science, Dammam, K.S.A.**
40. **Eid F and Al-Dossary A (2007):** Ultrastructural, histological and histochemical studies on the effect of electromagnetic field on the liver of pregnant rats and their fetuses. **The Egyptian Journal of Hospital Medicine,** 28: 273-294.
41. **El Salkh B (2009):** Histological and histochemical studies on the effect of the alternating magnetic field on the mice lung. **Egypt. J. Biomed. Sci.** (29): 351-366.
42. **George I, Ramesh k, Stem R, Chandrakasan G, et al (2001):** Dimethyl nitrosamine-induced liver injury in rats: the early deposition of collagen. **Journal of Toxicology.** 156: 129-138.
43. **Gu JW, Anand V, Shek EW, et al (1998):** Sodium induces hypertrophy of cultured myocardial myoblasts and vascular smooth muscle cell. **Journal of Hypertension.** 31:1083-1087.
44. **Nikolaos P, George Z, Nikolaos TP, Christos DG, Fevronia A, Nikolaos AM, et al (2004):** Thiol redox state (TRS) and oxidative stress in the mouse hippocampus after pentylenetetrazol–induced epileptic seizure. **Neurosci. Lett.** 357: 83-86.
45. **Willis C, Armario A, Piganini H, et al (2009):** Cholesterol and triglyceride concentration in rat plasma after stress. **Pharmacol. Biochem.Behav.** 31(1):75-79.
46. **Blumenthal M, Busse WR, Goldberg A, et al (2000):** The complete commission monographs. Therapeutic guide to herbal medicines .Boston ,M.A. **Integrative Medicines Communication.** 102: 80-81.
47. **Gorczyńska E and Wegryniewicz R (1991):** Structural and functional changes in organelles of liver cells on rat exposed to magnetic fields. **Environ. Res.** 55: 188-189.
48. **Cogger VC, Muller M, Fraser R, Khan J, et al (2004):** Effect of oxidative stress on the liver sieve. **J. Hepatology.** 41: 370-376.
49. **Goran B, Branko J, Vesna S, Katarina P, Jelena I, et al (2008):** Urban road –traffic noise and blood pressure and heart rate in preschool children. **Environment International.** 34: 226-231.
50. **Uran SL, Caceres LG, Guelman LR, et al (2010):** Effects of loud noise on hippocampal and cerebellar–related role of oxidative state. **Behavior Brain Research.** 1361: 102-114.



51. **El Habit O, Saada H, Azab K, Abdel-Rahman M, El Malah D, et al (2000):** The modifying effect of beta carotene on gamma radiation-induced elevation of oxidative reactions and genotoxicity in male rats. **Mut. Res.** 466: 179-190.
52. **Saada H and Azab K (2001):** Role of lycopene in recovery of radiation induced injury to mammalian cellular organelles. **J. Pharmazie.** 56(3): 239-240.
53. **Bunney GK (1992):** Agajanian, dopamine and norepinephrine inner- involvement of both dopaminergic and GABAergic components, vetted cells in the rat prefrontal cortex: pharmacological differentia. **Journal of Neuroscience.** 49: 857–865.
54. **Mark Pb, Bhashkar MB, Christopher L, Huangb K, et al (2001):** Detection of pharmacologically mediated changes in cerebral activity by functional magnetic resonance imaging: the effects of sulpiride in the brain of the anaesthetised rat. **Brain Research.** 916 : 107– 114.
55. **Braet F, Muller M, Vekeman K, Wisse E, Le DG, et al (2003):** Antimycin A-induced defenestration in rat hepatic sinusoidal endothelial cells. **Journal of Hematology.** 38: 394- 402.

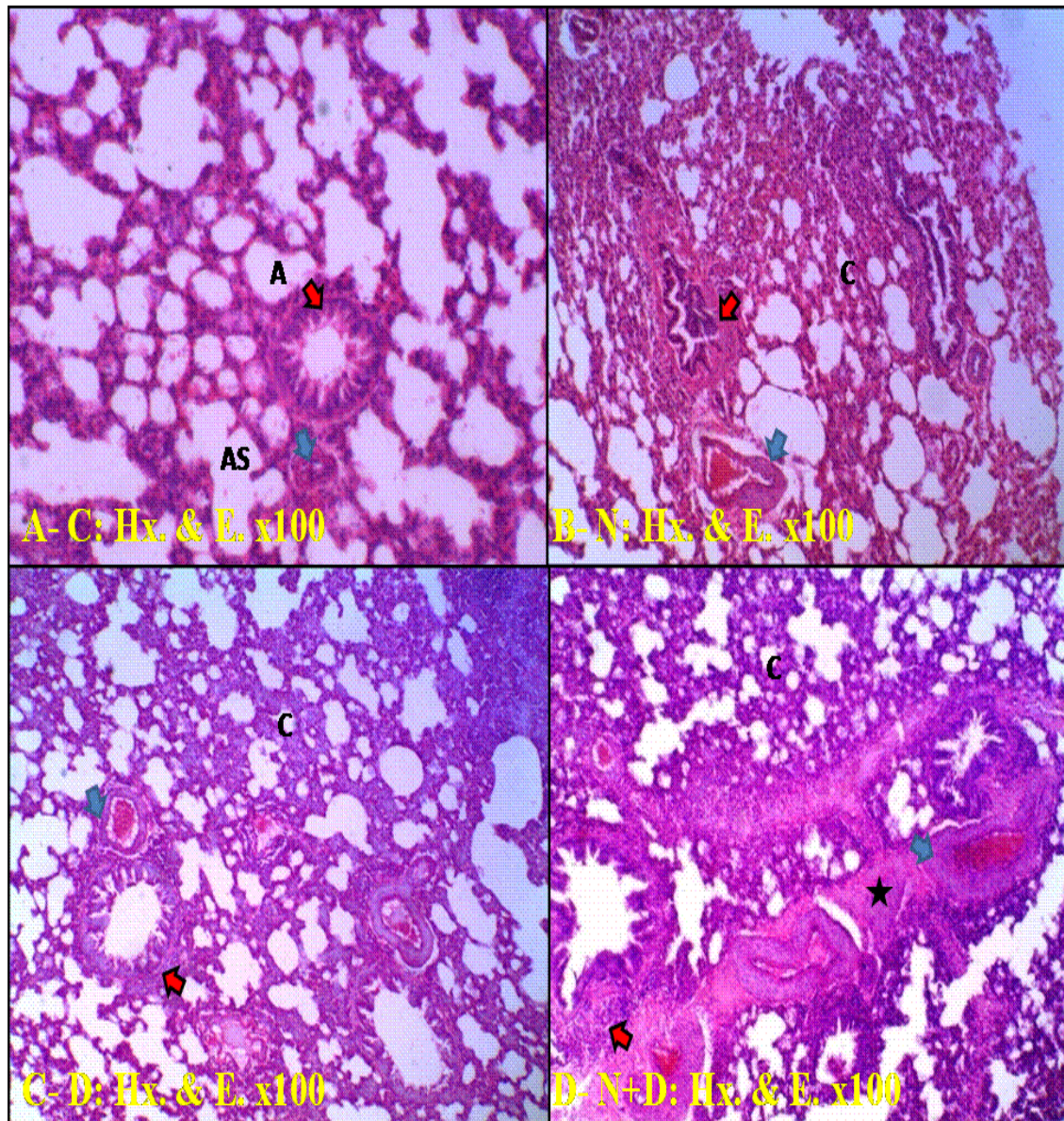


**Fig 1:** **A) Group 1** “Control rats” lung showing normal architecture of alveoli (A) with thin interalveolar septa, alveolar sacs (AS), bronchiole with highly folded columnar epithelial cells (red arrow) and normal pulmonary vessel (blue arrow). **B) Group 2** “Noise exposed rat” lung showing obliteration of some alveoli (c) with subsequent compensatory dilatation of others and thickened interalveolar septa. Numerous areas of cellular infiltration (red arrow) had been detected in the connective tissue surrounding lung bronchioles that showed elongated and corrugated walls. Thickened walls of the pulmonary blood vessels which contain haemorrhagic blood cells (blue arrow) are also detected. **C) Group 3** “Drug exposed rat” lung showing similar findings to noise exposed one. **D) Group 4** “Noise + Drug exposed rat” lung showing marked obliteration of some alveoli (c) and subsequent compensatory dilatation of others with thickened interalveolar septa. Marked thickening of bronchiole walls, peribronchiolar infiltration with inflammatory cells and granulomatous formation (red arrow) were detected. Moreover, thickened and congested pulmonary blood vessels (blue arrow) with marked perivascular infiltration and fibrosis (Black star) were detected ( **Hx. & E. x100**).



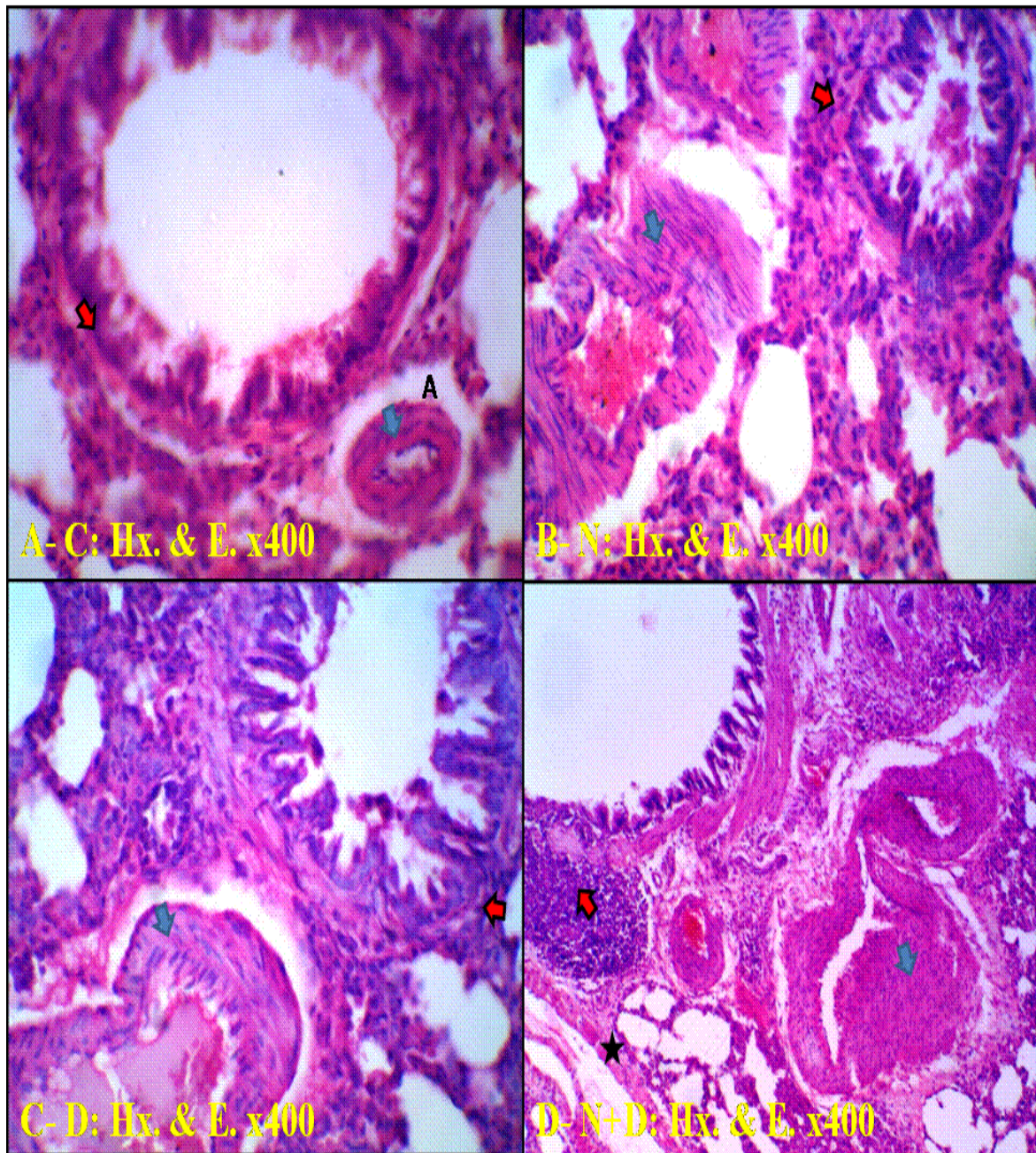


**Fig 2:** **A)** Group 1 “Control rats” lung showing normal architecture of alveoli (A) with thin interalveolar septa, bronchiole with highly folded columnar epithelial cells (red arrow) and normal pulmonary vessel (blue arrow). **B)** Group 2 “Noise exposed rat” lung showing obliteration of some alveoli with subsequent compensatory dilatation of others and thickening of interalveolar septa are observed. There is destruction in the surrounding bronchial muscle layer together with partial shedding of the mucosal lining, appearance of cellular debris in the destructed bronchiole and numerous areas of inflammatory cells infiltration in connective tissue surrounding lung bronchiole (red arrow). Thickened wall of the pulmonary blood vessels (blue arrow) which contain haemorrhagic blood cells is also detected. **C)** Group 3 “Drug exposed rat” lung showing somehow similar findings to noise exposed one. **D)** Group 4 “Noise + Drug exposed rat” lung showing marked obliteration of some alveoli with subsequent compensatory dilatation of others and thickening of interalveolar septa. Peribronchiolar inflammatory cells infiltration and granulomatous formation (red arrow) are also detected. Marked thickening of pulmonary blood vessels (blue arrow) is also detected with marked perivascular infiltration and fibrosis (Black star). (Hx. & E. x400).



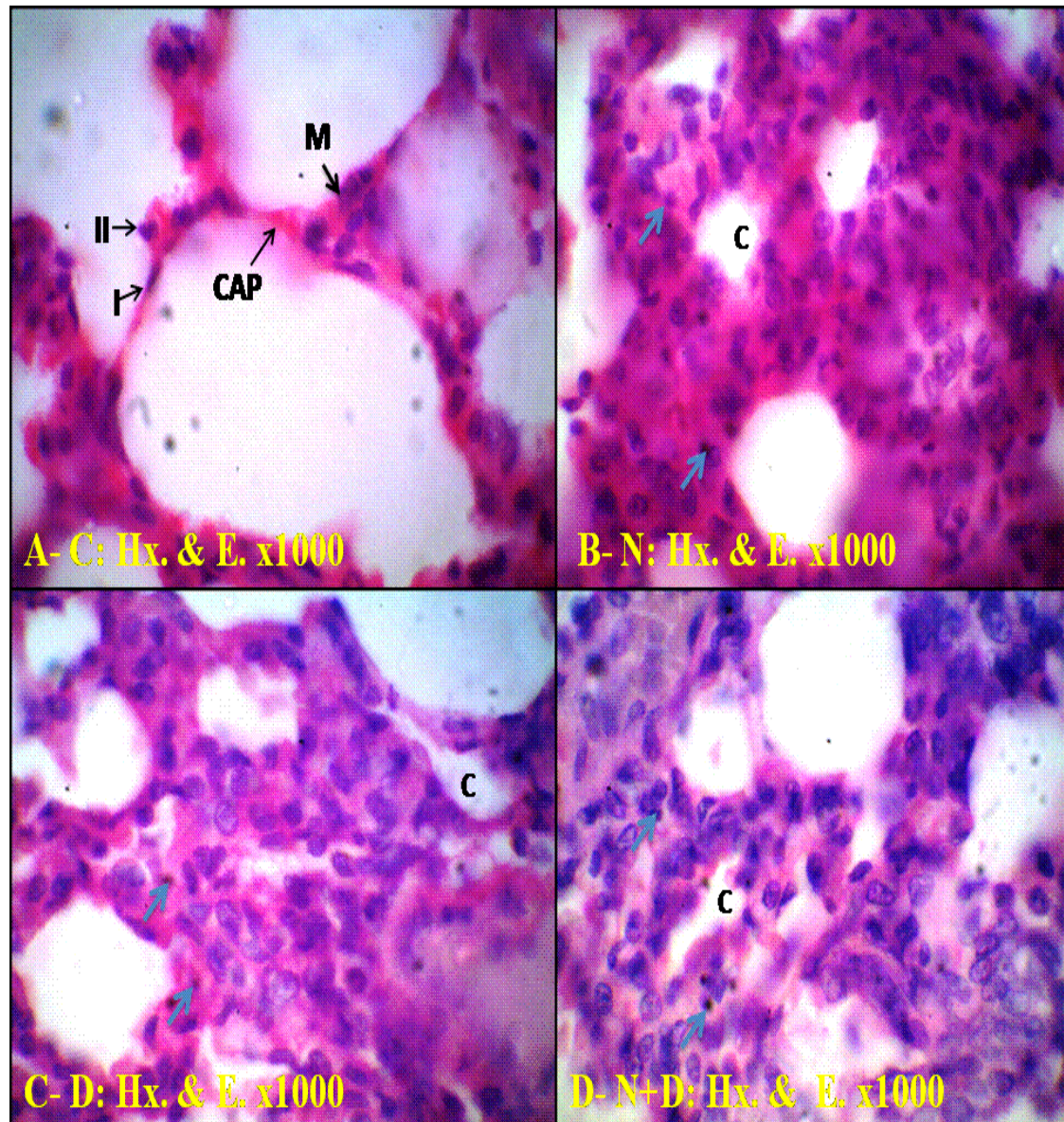


**Fig 3:**A) **Group 1** “Control rats” lung showing normal architecture of alveoli with thin interalveolar septa lined by type I pneumocyte (I) and type II pneumocyte (II), capillaries (CAP). Few number of macrophage cells (M) also detected in lung interstitium. **B) Group 2** “Noise exposed rat” lung showing collapsed alveoli (c) with compensatory expansion of other ones, thickening of interalveolar septa with massive infiltration of inflammatory cells. Cellular apoptotic changes are also detected (blue arrows). **C) Group 3** “Drug exposed rat” lung showing similar findings to noise exposed one. **D) Group 4** “Noise + Drug exposed rat” lung showing marked obliteration of some alveoli (c) with subsequent compensatory dilatation of others and in thickened interalveolar septa. Marked thickening of bronchiole wall with massive infiltration inflammatory cells and granulomatous formation around bronchiole are detected (red arrow). Cellular apoptotic changes (karyolysis and pyknosis) are also detected (blue arrows). (Hx. & E. x1000).



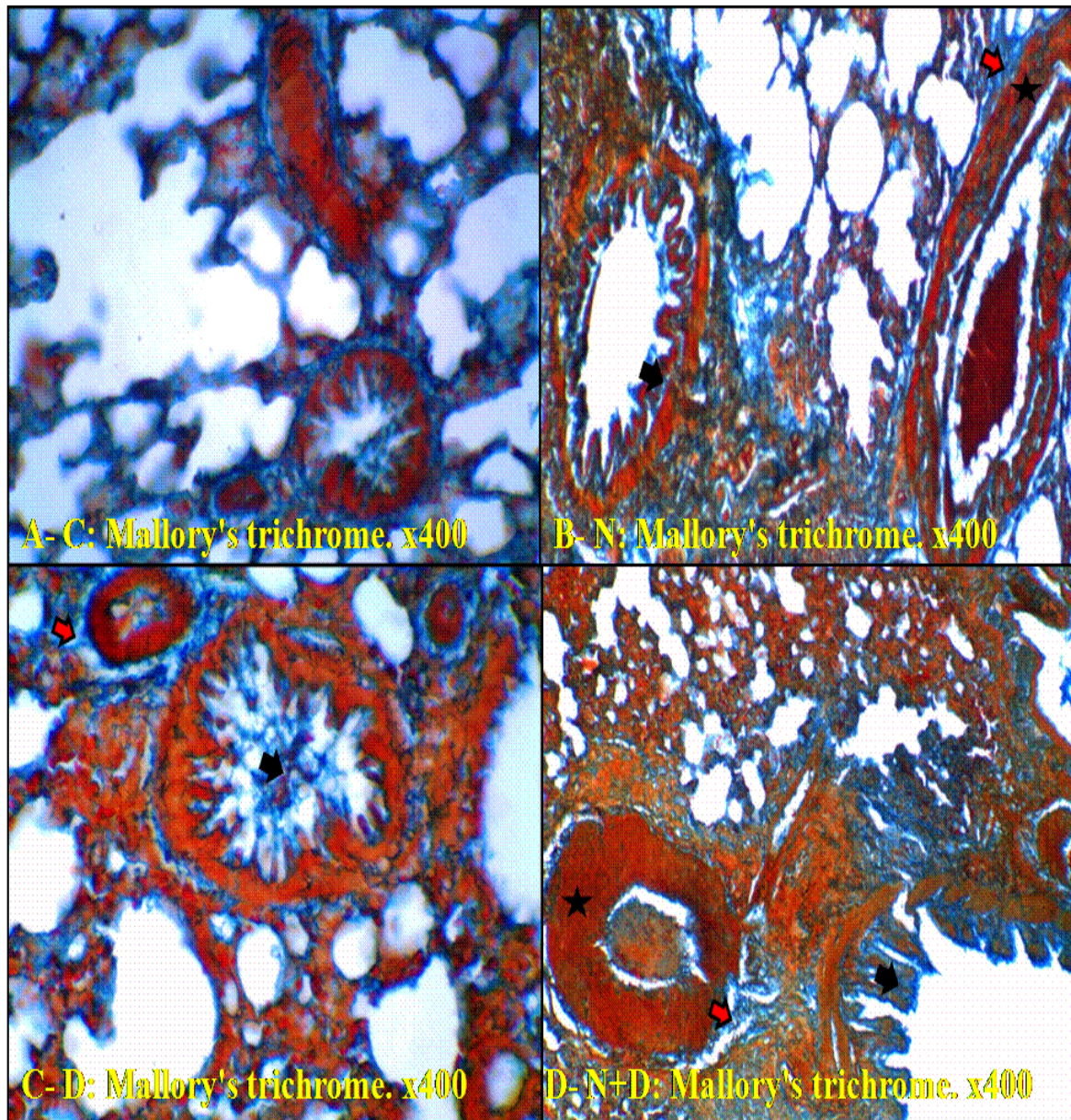


**Fig 4:** **A)** Group 1 “Control rats” lung showing normal distribution of collagen fibers in; pulmonary interstitium around the bronchioles, pulmonary blood vessels, alveolar sacs and in-between alveoli. **B)** Group 2 “Noise exposed rat” lung showing moderate amount of collagen fibers in the bronchiole submucosa, peribronchiolar area (black arrow) and in thick interalveolar septa with cellular infiltration in interalveolar septa. Areas of cellular infiltration are observed surrounding lung bronchiole. Moderate amount of collagen fibres are detected around the blood vessels (red arrow) with moderate thickening of the blood vessels (black star). **C)** Group 3 “Drug exposed rat” lung showing similar results to Group 2 with more collagen deposition around blood vessels (red arrow). Also, partial shedding of bronchiole mucosal lining was detected (black arrow). **D)** Group 4 “Noise + Drug exposed rat” lung showing marked amount of collagen fibers in bronchiole mucosa, submucosa (black arrow), peribronchiolar area and in thick interalveolar septa with cellular infiltration in interalveolar septa. Moderate amount of collagen fibres was detected around the blood vessels (red arrow) with marked thickening of blood vessels (black star). ( Mallory’s trichrome. x400).



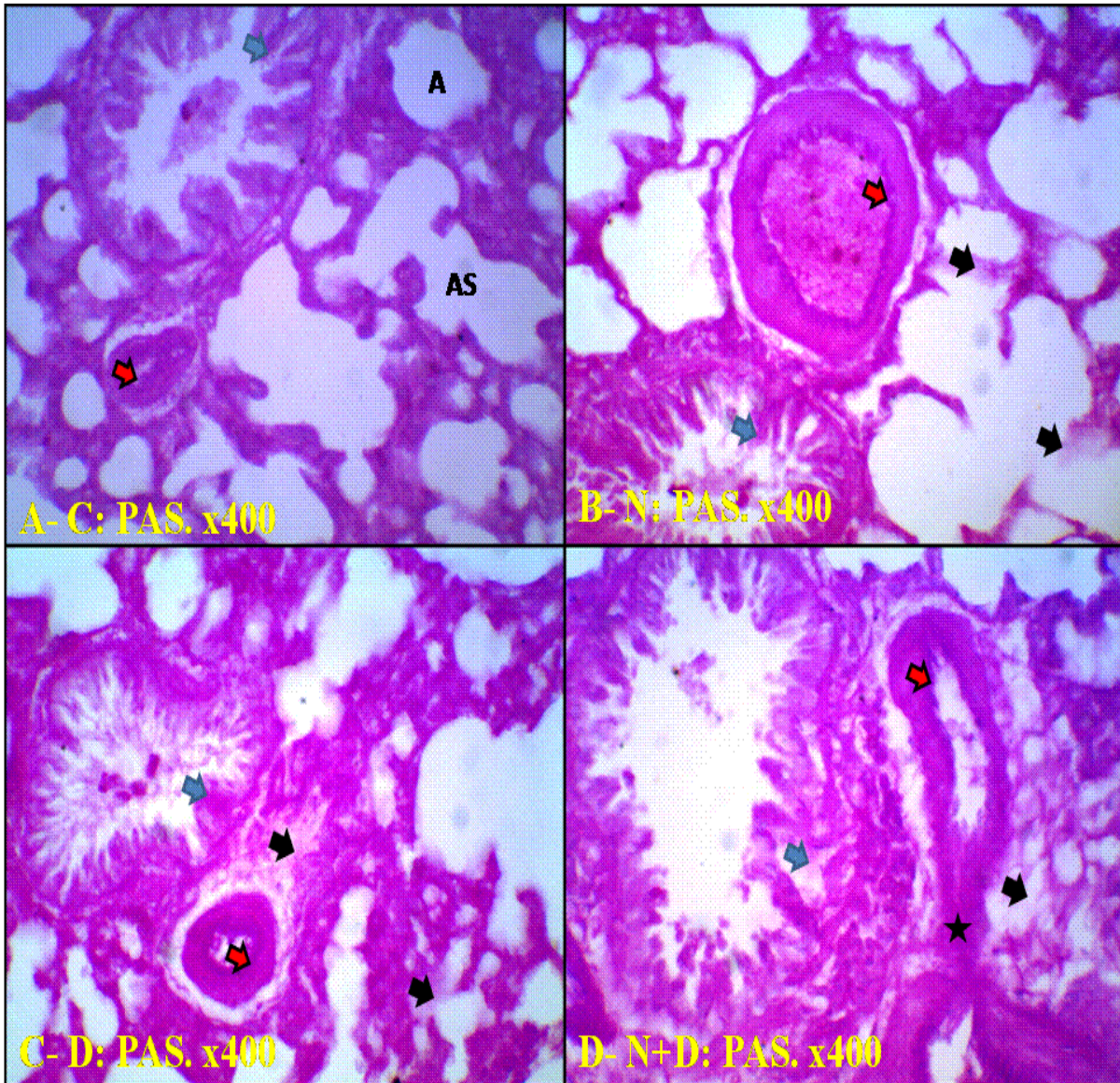


**Fig 5: A) Group 1** “Control rats” lung showing moderate PAS reaction (magenta red) in the basal lamina of the alveolar epithelium (A), alveolar sacs (AS), endothelium of pulmonary vessels (red arrows) as well as cytoplasm of epithelium lining bronchiole (blue arrow). **B) Group 2** “Noise exposed rat” lung showing strong PAS reaction in RBCs seen in the congested pulmonary vessels, in the endothelium of pulmonary vessels (red arrow) and in sites of interstitial cellular infiltration. Weak PAS reaction in alveolar epithelium, alveolar sacs (black arrow), shedded bronchiole epithelial cells (blue arrow) are observed. **C) Group 3** “Drug exposed rat” lung showing similar findings to noise exposed one. Also, weak PAS reaction is observed in perivascular area and collapsed alveoli (black arrow). **D) Group 4** “Noise + Drug exposed rat” lung showing strong PAS reaction in endothelium of pulmonary vessels (red arrow), in perivascular area (black star), and in sites of interstitial cellular infiltration. Also, weak PAS reaction is observed in perivascular area and collapsed alveoli (black arrow). (PAS.x400).



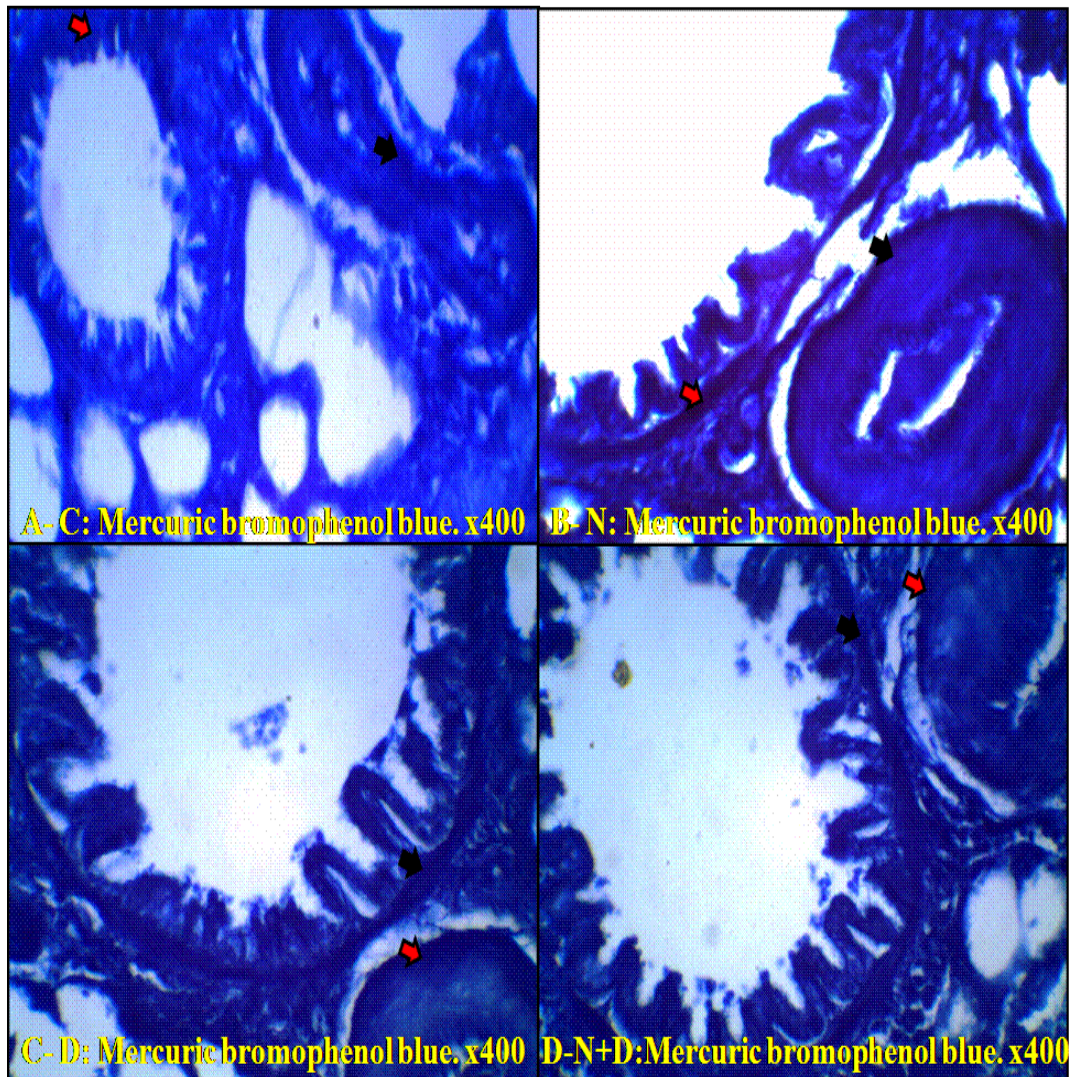


**Fig 6:** A) **Group 1** “Control rats” lung showing normal distribution of total protein in the pulmonary interstitium, in the muscular layer of bronchioles (red arrow) and the pulmonary blood vessels (black arrow). B) **Group 2** “Noise exposed rat” lung showing increased amount of total protein (deep staining) in the bronchioles (red arrow), peribronchiolar areas, and the thickened pulmonary blood vessels (black arrow). C) **Group 3** “Drug exposed rat” lung showing increased amount of total protein (deep staining) in the bronchioles (red arrow), peribronchiolar areas, and the thickened pulmonary blood vessels (black arrow). D) **Group 4** “Noise + Drug exposed rat” lung showing marked increased amount of total protein (deep staining) in the bronchioles (red arrow), peribronchiolar areas, and the thickened pulmonary blood vessels (black arrow). (Mercuric bromophenol blue. X400).



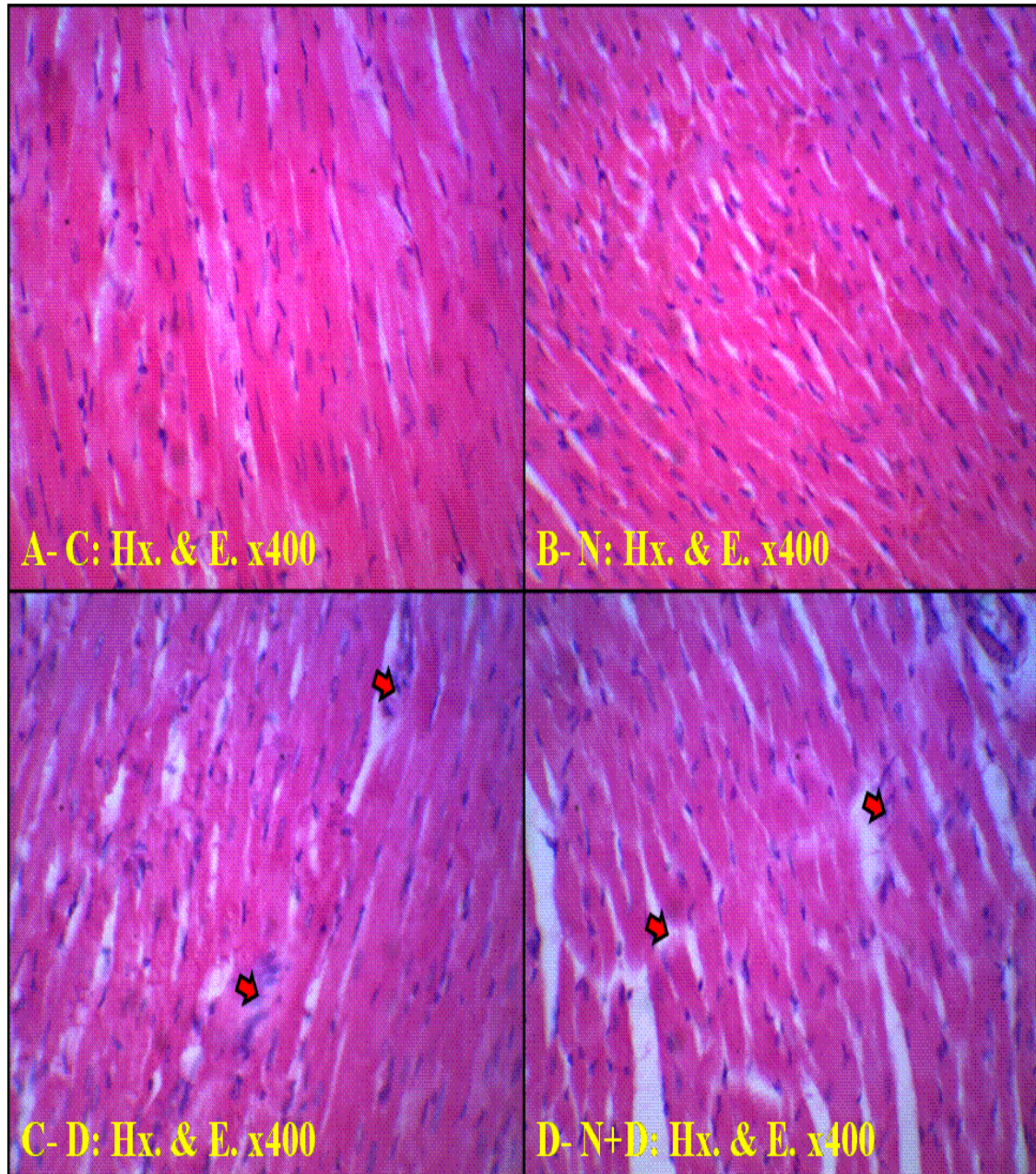


**Fig.7: A) Group 1** “Control rats” heart showing branching and anastomosing cardiac muscle fibers with acidophilic sarcoplasm and central elongated vesicular nuclei. **B) Group 2** “Noise exposed rat” heart showing some degenerative changes in myocardial fibres with numerous faintly stained nuclei. **C) Group 3** “Drug exposed rat” heart showing more myocardial cellular degenerative changes, inflammatory cells infiltration and widened endomysium than group 2. **D) Group 4** “Noise + Drug exposed rat” heart showing marked myocardial cellular degenerative changes and inflammatory cells infiltration with highly widened endomysium which contain debris of degenerated myocardial muscle fibres (red arrows). (Hx. & E. X400).



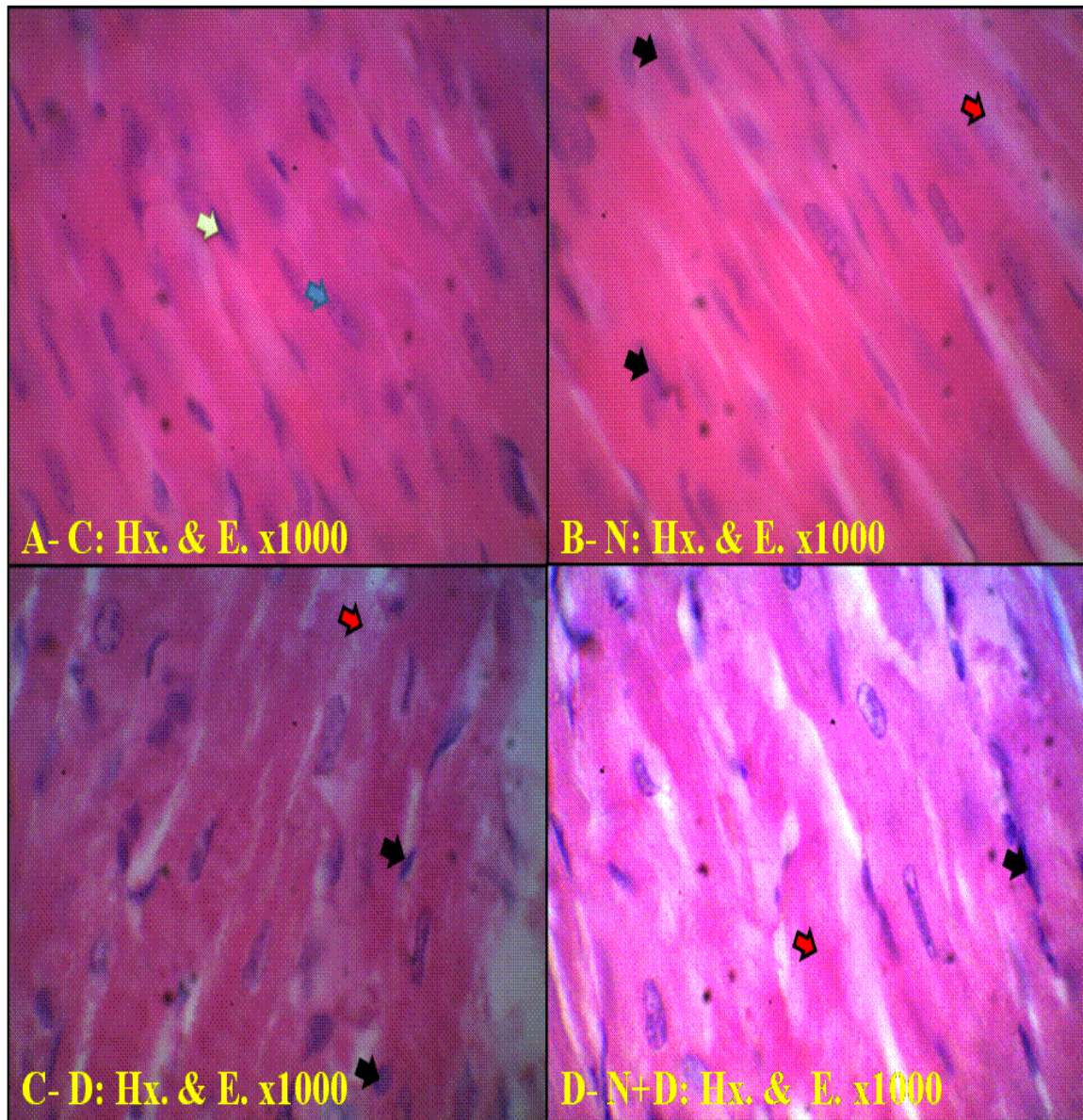


**Fig. 8: A) Group 1** “Control rats” heart showing branching and anastomosing cardiac muscle fibers with acidophilic sarcoplasm, vesicular nuclei of cardiomyocytes (blue arrow) and the nuclei of fibroblasts in the interstitium (yellow arrow). **B) Group 2** “Noise exposed rat” heart showing focal areas of necrotic fibres with vacuolated cytoplasm (red arrow) and small deeply stained pyknotic nuclei (black arrow). **C) Group 3** “Drug exposed rat” heart showing focal areas of necrotic fibres with vacuolated cytoplasm (red arrow) and small deeply stained pyknotic nuclei (black arrow). **D) Group 4** “Noise + Drug exposed rat” heart showing more necrotic (red arrow) and cellular karyolytic changes (black arrow) than group 2 & 3. (Hx. & E. x1000).



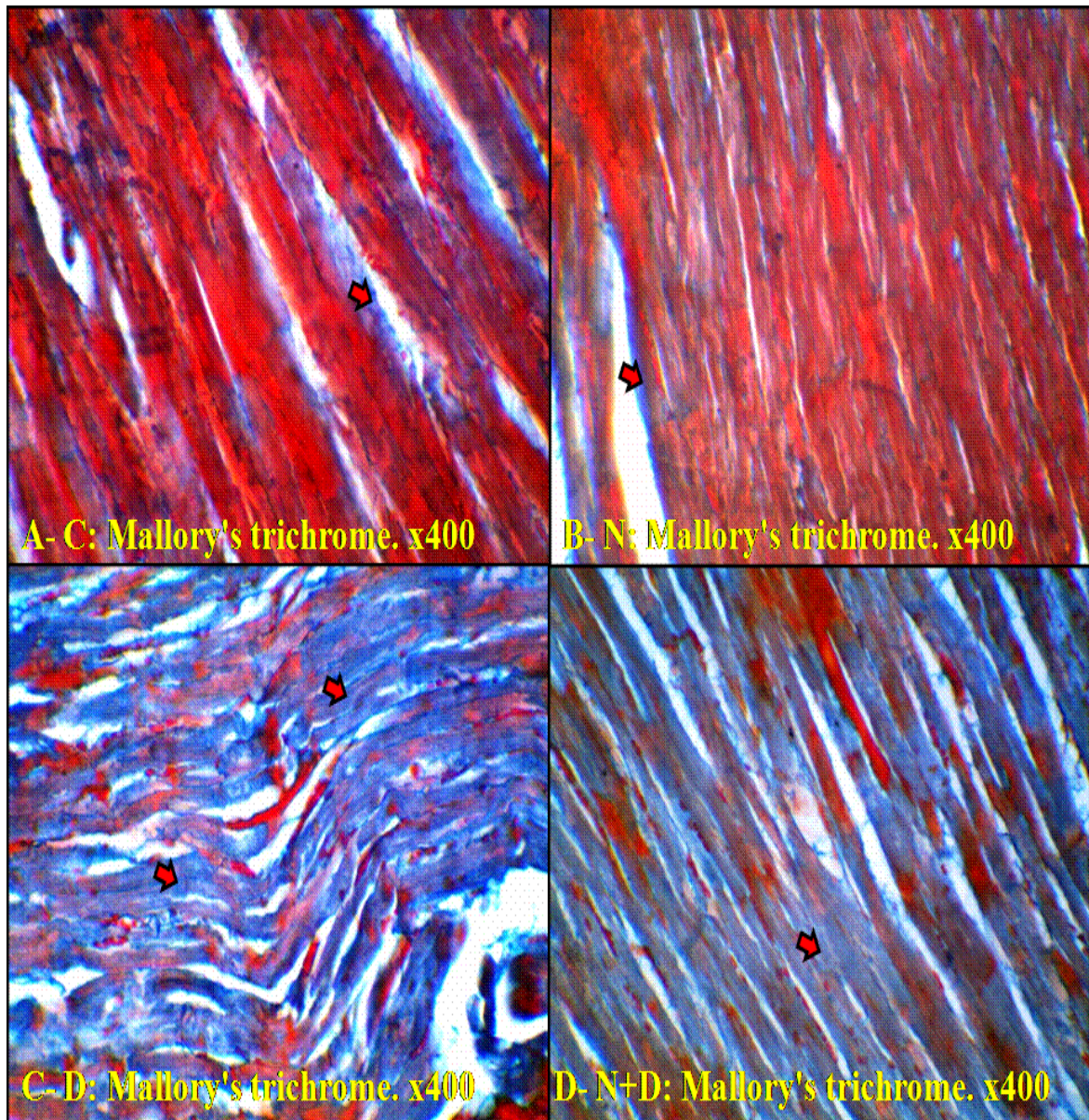


**Fig 9:**A) Group 1 “Control rats” heart showing few collagen fibers inbetween the cardiac muscle fibers (red arrow). B) Group 2 “Noise exposed rat” heart showing few collagen fibers inbetween the muscle fibers (red arrow) and no difference is detected in comparison to the control group. C) Group 3 “Drug exposed rat” heart showing highly increase in collage muscle fibres deposition in comparison to control group (red arrow). D) Group 4 “Noise + Drug exposed rat” heart showing marked increase of the collage muscle fibres deposition in comparison to the control group (red arrow). (Mallory’s trichrome. x400).



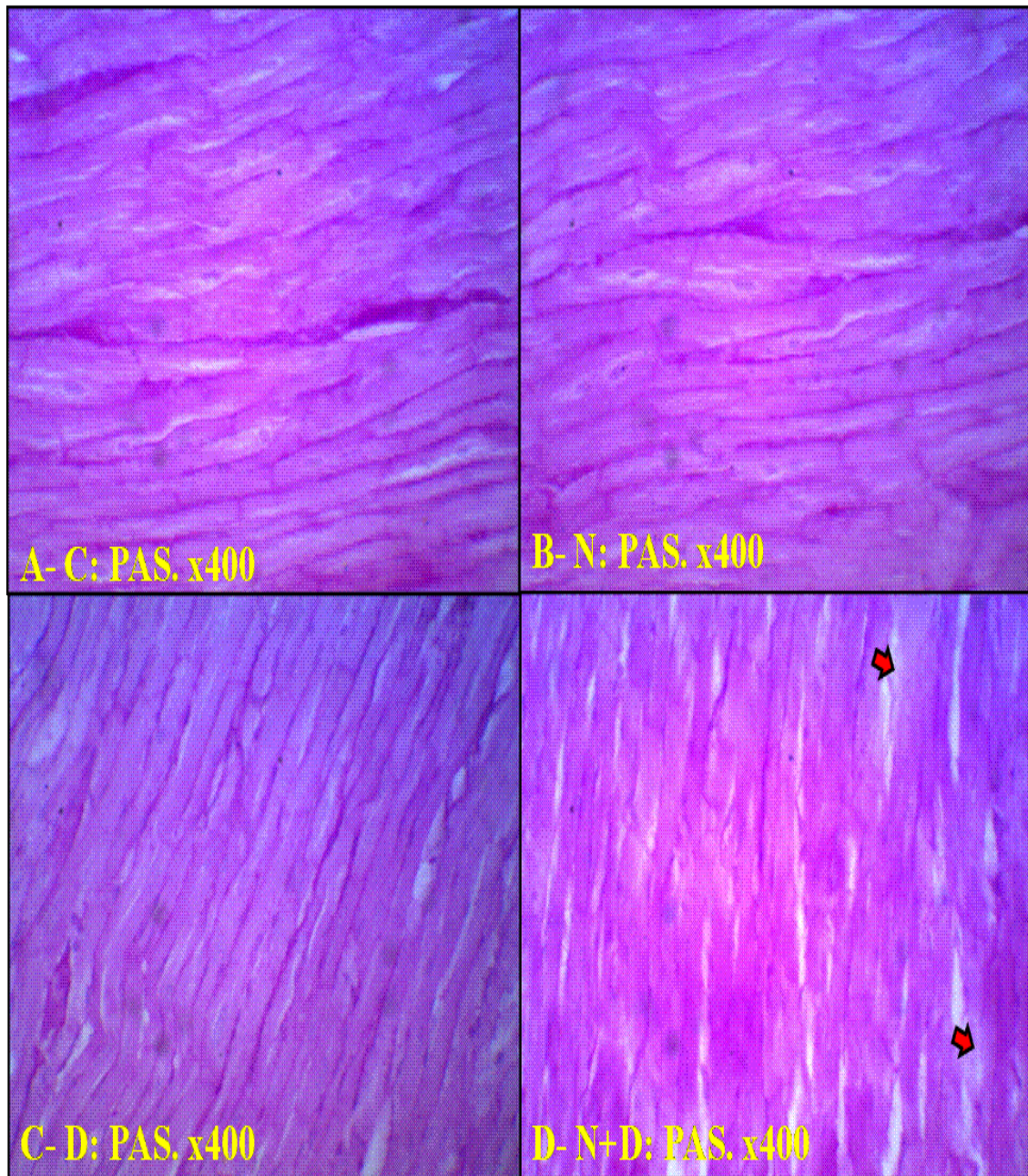


**Fig 10:** A) **Group 1** “Control rats” heart showing normal polysaccharides content (normal distribution of PAS +ve materials) in the cardiac myocytes. B) **Group 2** “Noise exposed rat” heart showing normal polysaccharides content (normal distribution of PAS +ve materials) in the cardiac myocytes. C) **Group 3** “Drug exposed rat” heart showing normal polysaccharides content (normal distribution of PAS +ve materials) in the cardiac myocytes. D) **Group 4** “Noise + Drug exposed rat” heart showing poorly stained (focal areas of decreased affinity of PAS stain) cardiac myocytes (red arrow). (PAS. x400).



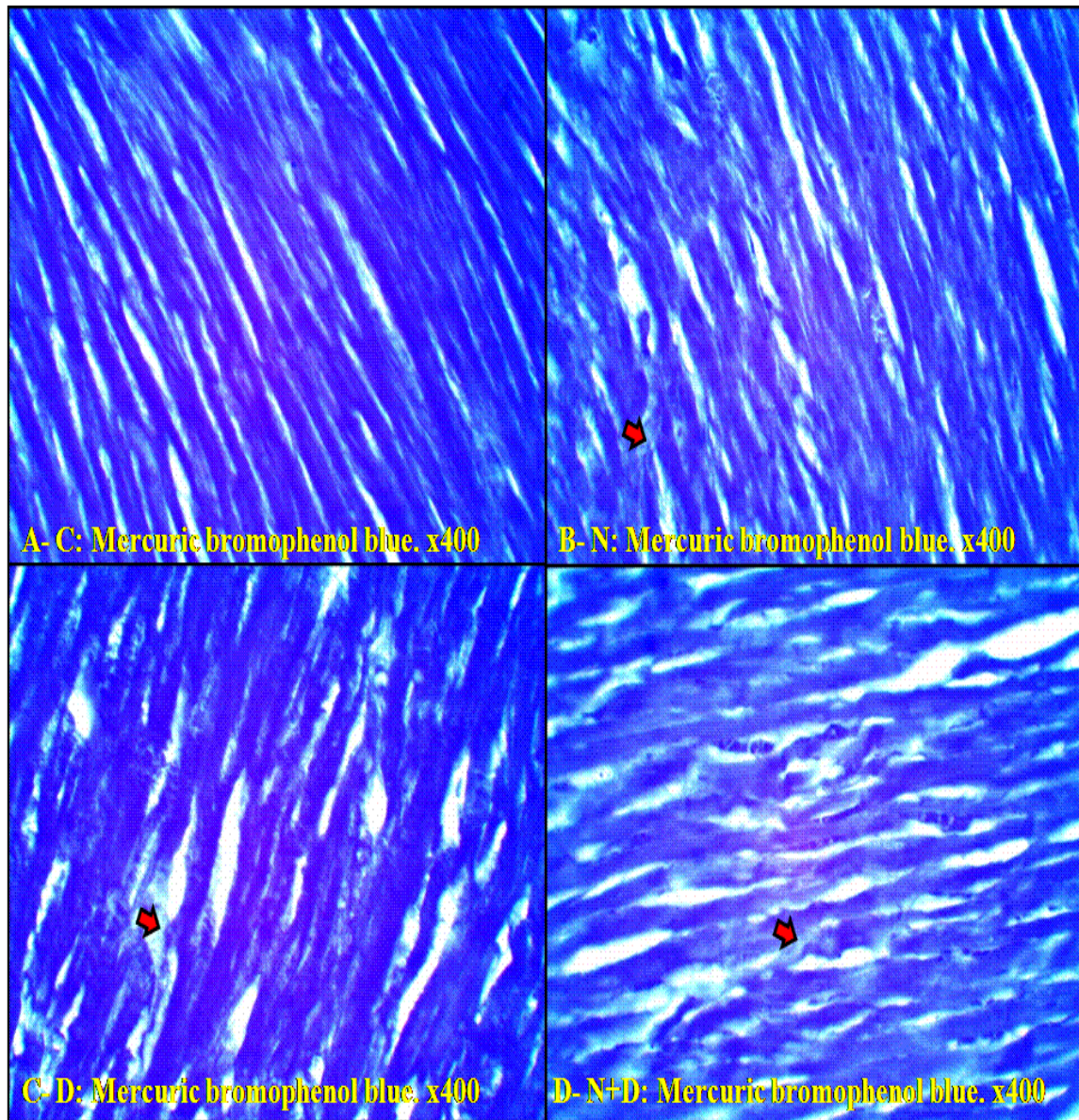


**Fig 11: A) Group 1** “Control rats” heart showing normal distribution of total protein in the cardiac myocytes. **B) Group 2** “Noise exposed rat” heart showing reduced total protein (focal areas of fainting stain) content in cardiac myocytes (red arrow). **C) Group 3** “Drug exposed rat” heart showing reduced total protein (focal areas of fainting stain) content in cardiac myocytes (red arrow). **D) Group 4** “Noise + Drug exposed rat” heart showing marked reduction in total protein (fainting stain) content in the cardiac myocytes (red arrow).(Mercuric bromophenol blue. x400).

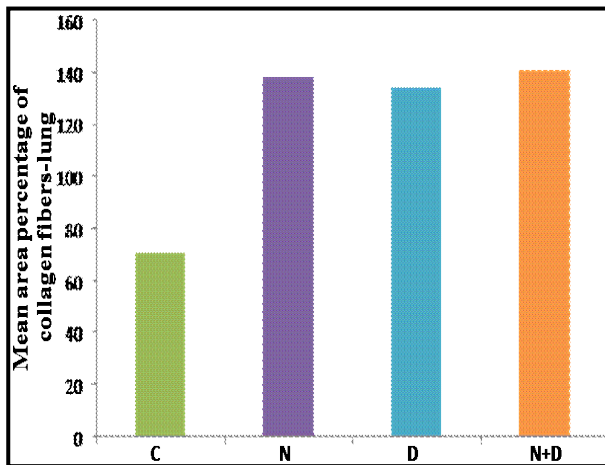


**Fig 12:** Mean thickness of interalveolar septa in lungs of the different groups of the study.

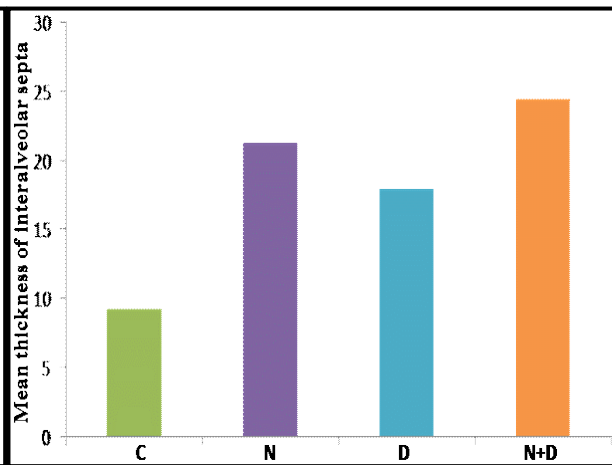


**Fig 13:** Mean area percentage of collagen fibres in lungs of the different groups of the study.

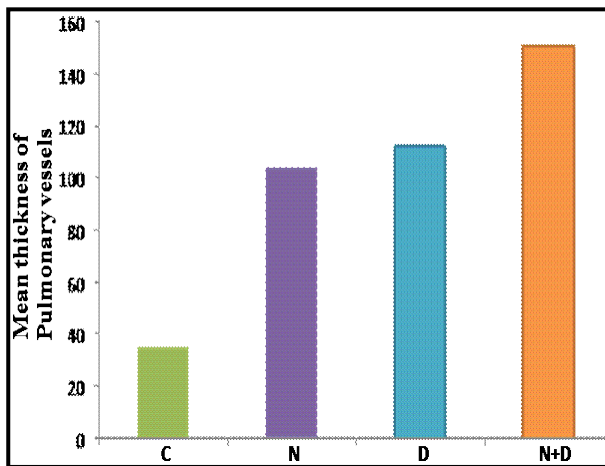


**Fig 14:** Mean number of alveolar macrophages in lung of the different groups of the study.

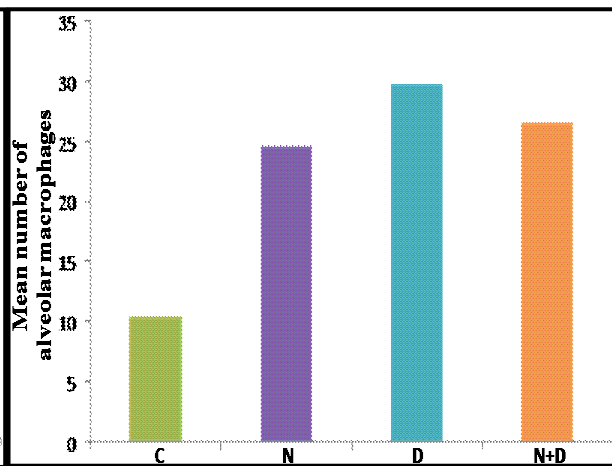


**Fig 15:** Mean thickness of pulmonary vessels in lungs of the different groups of the study.

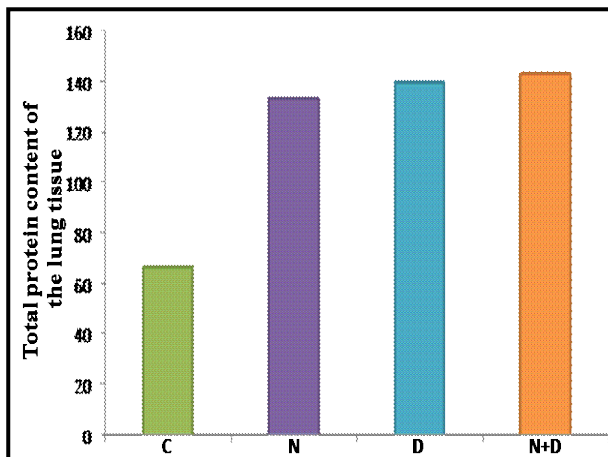


**Fig 16:** Total protein in lung tissue of the different groups of the study.

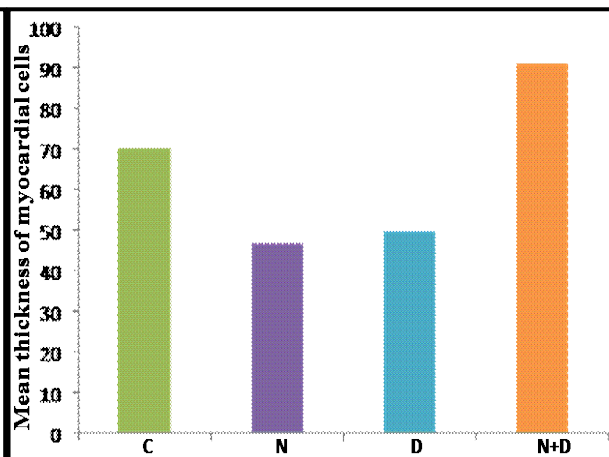


**Fig 17:** Mean thickness of myocardial cells in heart of the different groups of the study.

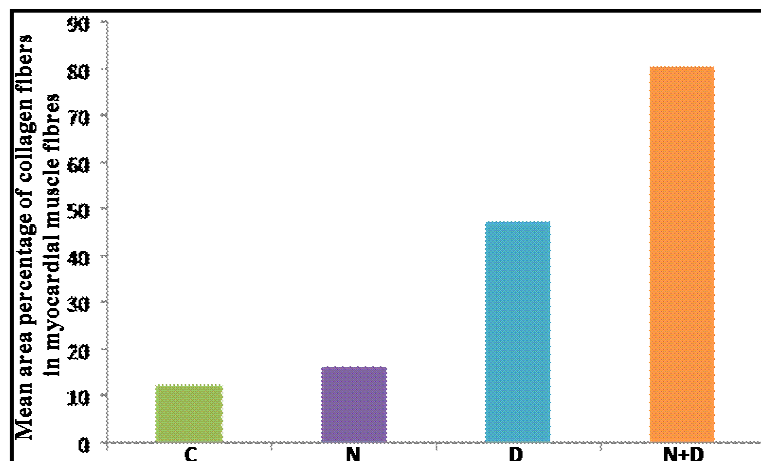


**Fig 18:** Mean area percentage of collagen fibres in myocardial muscle fibres of the different groups of the study.

Study group	Mean thickness of the interalveolar septa $\pm$ SD	Mean number of the alveolar macrophages $\pm$ SD	Percentage of collagen fibres in the lung alveoli $\pm$ SD	Mean thickness of the pulmonary vessels $\pm$ SD	Total protein in lung tissue $\pm$ SD	Mean thickness of the myocardial muscle fibres $\pm$ SD	Percentage of collagen fibres in the myocardial muscle fibres $\pm$ SD
Group 1 (C)	9.25 $\pm$ 2.31	10.4 $\pm$ 1.14	70.77 $\pm$ 17.15	35.21 $\pm$ 8.58	66.27 $\pm$ 12.14	70.17 $\pm$ 16.69	12.22 $\pm$ 3.38
Group 2 (N)	21.32 $\pm$ 6.41**	24.6 $\pm$ 2.07*	138.55 $\pm$ 23.82**	104.49 $\pm$ 35.23**	133.35 $\pm$ 13.32**	46.73 $\pm$ 11.83**	16.17 $\pm$ 3.91
Group 3 (D)	17.93 $\pm$ 3.76**	29.8 $\pm$ 2.16*	133.98 $\pm$ 30.27**	112.83 $\pm$ 14.01**	139.68 $\pm$ 32.17**	49.69 $\pm$ 10.72**	47.28 $\pm$ 5.37**
Group 4 (N + D)	24.43 $\pm$ 8.01**	26.6 $\pm$ 1.82*	141.27 $\pm$ 34.87**	151.01 $\pm$ 79.29**	143.23 $\pm$ 14.87**	90.98 $\pm$ 11.76	80.56 $\pm$ 17.1**

**Tab 1: Thickness of interalveolar septa, number of alveolar macrophages, percentage of collagen fibres in the lung alveoli, thickness of the pulmonary vessels, thickness of the myocardial muscle fibres and percentage of collagen fibres in the myocardial muscle fibres of the different groups of the study expressed as mean  $\pm$  SD.**

\*indicates significant difference from the control group ( $P < 0.05$ ).

\*\*indicates highly significant difference from the control group ( $P < 0.001$ ).